

The electronic structure of solid surfaces*

Joel A. Appelbaum and D. R. Hamann

Bell Laboratories, Murray Hill, New Jersey 07974

We present a short review of the current status of electronic structure calculations for ordered solid surfaces. For the s - p bonded metal surfaces, emphasis is centered entirely on self-consistent field (SCF) calculations employing a local density approximation for exchange and correlation. For semiconductor surfaces both SCF and empirical tight-binding methods are discussed, while for transition metal surfaces, where no SCF calculations have been carried out, a number of different schemes for solving Schrödinger's equation at a surface are reviewed that use plausible but not self-consistent forms for the surface potential. Finally, calculations for chemisorbed systems are briefly covered, with emphasis on ordered monolayers on semiconductor and transition metal surfaces.

CONTENTS

I. Introduction	479
A. Scope	479
B. Basic concepts	480
II. s - p bonded metals	483
A. Jellium	483
B. Sodium	485
C. Lithium	486
D. Aluminum	486
III. Semiconductors	487
A. Si(111)1×1	487
B. Si(111)2×1	488
C. Si(100)2×1	490
D. Polar semiconductors	490
IV. Transition metals	492
A. Cu	492
B. W and Mo	492
C. Fe(100)	492
V. Chemisorption	493
A. Introduction	493
B. H on Si(111)	493
C. O on Ni(100)	494
VI. Summary	494
References	495

I. INTRODUCTION

A. Scope

The electronic structure of solid surfaces has become a very active area of study in the past few years. Recent advances in experimental techniques have produced an abundant supply of reliable data on clean, well-ordered single crystal surfaces (Eastman and Nathan, 1975; Park, 1975; Plummer *et al.*, 1975). This, in turn, has spurred theoretical research in the development and application of models and computational techniques (Schrieffer and Soven, 1975). To attempt a comprehensive review in this rapidly developing area seems somewhat premature. Instead, this survey is aimed at presenting the authors' selection of a sampling of recent work that seems to offer the most promise for further development and application.

The scope of this review is limited to theoretical

*This paper is adapted from one to appear in CRC Critical Reviews in Solid State Physics as part of a series of papers that were presented at the Second International Summer Institute in Surface Science, held at the University of Wisconsin, Milwaukee, 18-22 August 1975. The complete proceedings of the Institute appear in this volume.

studies of the electronic structure of solid surfaces in the independent-particle approximation. Explicitly collective effects, such as surface plasma oscillations, are excluded. Interest is further focused on the occupied electron states, and low-lying excited states which are still bound within the solid. This excludes the considerable literature concerned with the diffraction of low-energy electrons (30 to 300 eV) from surfaces (LEED). While many formal parallels exist between this problem and that of the occupied states, a quite different set of physical effects is emphasized in each case. For example, in LEED the strong potential in the core regions of atoms in the vicinity of the surface is of primary importance, while for the valence states, the bonding potential between atoms is paramount. In addition, LEED electrons have a short mean free path (5-10 Å) between inelastic collisions, and this fact plays an important role in most calculational techniques developed in this field. Ground state one-electron wave functions are, of course, not subject to decay.

Another criterion for selection was that the work reviewed pertain explicitly to extended surfaces. Calculational techniques developed for molecular problems have recently been applied to clusters of atoms as a means to study surface electronic structure. The question of what aspects of such results apply to extended surfaces remains largely unexplored at present, however.

The final criterion consciously applied in arriving at the presented selection of work is one of realism. A wide range of simplified models have been devised to explore various aspects of surface electronic structure qualitatively. The recent trend, however, is towards models representing specific solids and their surfaces well enough to permit quantitative comparisons with experimental studies. Such calculations have now been carried out for simple metals, semiconductors, transition metals, and surfaces with chemisorbed overlayers. The methods employed range from empirical to first principles in nature, and the questions investigated range from demonstrating the existence of an isolated surface state to determining the complete spectrum, geometry, and charge distribution. Earlier work treating more simplified models has been reviewed by Davison and Levine (1970) and by Jones (1975).

The material in this review is organized as follows. In the second subsection of this Introduction, general concepts underlying the description of surface electronic structure are discussed. Many of these are often taken

for granted in the literature, and this summary is intended to provide a base from which the nonspecialist can approach the literature. No specific results are discussed, and no references are given. The remaining material is grouped according to the physical system treated rather than the methods employed. Examples of studies of simple metals (those with s - p bonding) are given in Sec. II. Studies of semiconductors, transition metals, and chemisorbed overlayers are given in Secs. III, IV, and V, respectively. While there is some grouping of methods employed with systems treated, there is considerable overlap. A method is discussed in detail when it is first introduced, and reference is made to this discussion when it appears in subsequent sections.

The emphasis in Secs. II to V is twofold. On the one hand, we wish to provide a sufficiently detailed picture of the physical approximations involved in each model to enable the reader to establish his own credibility limits, and to give some indication of the complexity and completeness of the calculation. On the other hand, we wish to stress the nature of the physical problems being explored and consequently have made reference to the experimental literature where appropriate. In no sense, however, should our limited citations be regarded as a review of the experimental literature, even on the specific subject in question.

Section VI gives a brief summary and indicates our expectations for the continuing evolution of this field and the factors which will shape this evolution.

B. Basic concepts

While we must assume that the reader has at least a passing familiarity with common concepts and calculational techniques in the electronic structure of bulk solids, a few general concepts related to surface electronic structure will be introduced below. Many of these will be expanded upon in more detail in the context of specific calculations described later.

A basic concept underlying the entire subject of this review is that of the surface region, which refers to the volume of space containing the last few atomic layers of the solid, any adsorbed overlayers if present, and the nearby vacuum.¹ In this region, the atomic geometry may depart from that of the bulk, and the effective potential seen by the electrons changes from that characteristic of the bulk to the constant vacuum level. While this is the "physical" definition of the surface region, the working definition differs with calculational technique and depends on the approximations made. These may range from neglecting the surface region altogether by assuming that the bulk abruptly joins the vacuum, to letting the surface region include the entire system, as might be done in the case of a slab calculation (a finite number of atom layers with two surfaces).

Another working definition of the surface region can be made on the basis of experimental techniques. The

two most commonly applied probes of the surface spectrum are ultraviolet photoemission spectroscopy and inelastic low-energy electron scattering. Both techniques derive their surface sensitivity from the fact that the mean free path of the electrons involved in each is quite short, say 5–10 Å. These spectroscopies thus selectively probe the first few atom layers. While a detailed calculation of the entire process involved in each type of spectroscopy is ultimately desirable for theoretical comparison, the simpler alternative usually adopted is to assume that structure seen in these spectroscopies is characteristic of the surface density of states. The local density of states is a well-defined theoretical concept. It is simply the total density of states for the system weighted by the squared magnitude of the wave functions in an incremental energy range at the spatial point in question. The local density of states integrated over the surface region, possibly with a weighting factor that decays towards the bulk, is the sort of output that might be generated by a theoretical study and called the surface density of states in a sense paralleling the experimental definition.

As a consequence of the three-dimensional periodicity of a bulk solid, electron eigenstates can be classified by a Bloch wave vector \vec{k} uniquely defined within the Brillouin zone. The presence of a surface destroys periodicity in the direction normal to the surface, but periodicity in the directions parallel to the surface remains. The electron states in the presence of a surface can thus be characterized by a two-dimensional Bloch wave vector $\vec{k}_{||}$, which is uniquely defined within a polygon that is the surface Brillouin zone. The bulk band structure can be projected onto the surface Brillouin zone. For each $\vec{k}_{||}$, there will be continuous ranges of energies for which bulk states exist and gaps in which no bulk states exist. The presence of a low-index surface will usually leave some symmetry operations possessed by the bulk solid intact, and the system will belong to some point group involving rotations about the surface normal and reflections in planes containing the surface normal. For wave vectors $\vec{k}_{||}$ that are invariant under some subgroup of this point group, states may be further classified as belonging to various irreducible representations of the subgroup. States belonging to different representations will not mix. In projecting the bulk band structure onto $\vec{k}_{||}$'s which lie at symmetry points of the surface Brillouin zone, allowed energy ranges and gaps may be similarly classed by symmetry type. It is perfectly possible to have an allowed region for one symmetry type overlap a gap for another.

Suppose the band structure problem is turned around and considered from the point of view of the surface classification of states. Given a $\vec{k}_{||}$, an energy E , and a symmetry type if appropriate, what are the solutions of Schrödinger's equation for the bulk potential that are periodic in the direction normal to the surface (which we shall call the z direction)? If E falls in one of the aforementioned allowed ranges, there are of course one or more pairs of Bloch states with wave vectors $k_z^{\pm}(E)$. There are, in addition, an *infinite* number of solutions with *complex* k_z . These are the so-called evanescent Bloch waves, and they are normally neglected in dealing

¹The term surface is also used in a more restricted sense to refer to the last atomic layer, with the term seldge employed for additional nearby layers that are perturbed by the surface.

with a bulk solid since they diverge in amplitude as z goes to either $+\infty$ or $-\infty$. In the presence of the surface, however, evanescent waves that decay into the bulk are perfectly permissible components of a wave function. While an infinite number of evanescent waves exist in principle for any \vec{k}_{\parallel} and E , a calculation with a finite basis will only give a finite number, related to the number of bands. Any given complex $k_z(E)$ can be followed as a function of energy; each will become real for a certain range of energy. Thus each evanescent wave can be considered to "belong" to a band of propagating waves. In general, only evanescent waves belonging to bands near a given energy will play any significant role in wave functions at that energy for the solid with its surface.

Outside the surface region in the vacuum, the electron wave functions with which we shall be concerned are decaying exponential functions with periodic modulation parallel to the surface. In the surface region itself, the potential lacks any simple description aside from its two-dimensional periodicity, and there is nothing one can say about the electron states other than specifying \vec{k}_{\parallel} and E .

There are two distinct types of wave functions that must be considered in any complete study of surface electronic structure. For a given \vec{k}_{\parallel} and any E in an allowed band, there will be one or more scattering states. These are specified by the requirement that deep in the bulk they consist of a single propagating Bloch wave carrying current toward the surface, and one or more reflected Bloch waves. In calculating the total charge or density of states, the incident Bloch waves are conventionally normalized (to one electron per bulk unit cell), are summed over occupied bands, and are integrated over the three-dimensional bulk Brillouin zone, assigning equal weight to equal volume elements for the three-dimensional Bloch vector \vec{k} . The other type of wave functions which must be considered are those of surface states. These can exist for particular energies which lie in the gaps or forbidden regions for a given \vec{k}_{\parallel} . They consist purely of decaying evanescent waves in the bulk, and thus are "bound" to the surface. The existence of one or more surface states in a gap depends on the detailed nature of the potential in the surface region, and cannot be in general predicted in the absence of this information. Once a surface state is known to exist at a given \vec{k}_{\parallel} in a certain gap, one can attempt to follow it as a function of \vec{k}_{\parallel} and thereby define its dispersion relation $\epsilon(\vec{k}_{\parallel})$. Several things may happen: The gap and the surface state may exist over the entire surface Brillouin zone; the gap may close up and "squeeze out" the surface state; or the surface state $\epsilon(\vec{k}_{\parallel})$ may merge into the allowed band at an edge of the gap and the surface state disappear while the gap persists. A related question concerns the extent of localization of charge in a surface state, that is, the apportionment of its charge between the surface region and its evanescent tail in the bulk. Typically, a surface state near the center of a wide gap will be highly localized in the surface region, while one in a small gap or with its energy near the edge of a gap will have a lot of its weight in a slowly decaying tail. Thus a state merging into the edge of a gap

might gradually fade away in terms of its amplitude at the surface, rather than abruptly vanish.

Another situation may exist that, while it involves scattering states, is closely related to the formation of surface states. This is the so-called surface resonance. If one plots the squared amplitude of a scattering state integrated over the surface region while sweeping the energy E across an allowed band (fixed \vec{k}_{\parallel}), it will typically vary smoothly and go to zero at the band edges. In some circumstances, however, it may be sharply peaked about a particular energy, with the integrated charge under the peak equal to a sizeable fraction of an electron in the surface region. This might occur, for example, at the edge of a band if the disturbance in the surface region is not quite strong enough to split off a surface state from that band. Another situation in which one finds resonances is when a surface state split well below one minimum in the band structure (in the sense that the principal component of its evanescent tail "belongs" to that minimum) runs into another overlapping band. In this case, a surface state one was following as a function of \vec{k}_{\parallel} would not "fade away" as it approached the edge of the "foreign" band, but keep its charge more or less intact and acquire some small width in energy. In such a situation it is conceptually valid to regard the $\epsilon(\vec{k}_{\parallel})$ relation as extending into the band region. Another situation in which a sharp resonance might be expected is when a well-localized surface state at a symmetry point in the surface Brillouin zone is overlapped by a band of a different symmetry. As one moves away from the symmetry point in certain directions, the surface state and the band will be mixed by the symmetry-breaking component of \vec{k}_{\parallel} . The mixing may be sufficiently weak over a considerable region that it is valid to associate a surface state-like $\epsilon(\vec{k}_{\parallel})$ with the resonance, even though a true surface state only exists at a single point or on a single line.

There is a good reason behind the emphasis that has been placed on surface states, surface resonances, and their $\epsilon(\vec{k}_{\parallel})$ dispersion relation in the preceding discussion and in much of the literature. It is that the most interesting and experimentally accessible features of the surface density of states will be those arising from the surface state. The two-dimensional dispersion relation can have critical points that give rise to steps and to logarithmic singularities in the density of states. This is sharper structure than that attained by the bulk density of states. In addition, the appearance of surface states is related to differences between the surface and the bulk, and the presence or absence of surface-state related structure in a spectrum can yield information to test various hypotheses about changes in geometry and chemical bonding at the surface. While the contributions of nonresonant scattering states to the surface density of states will certainly reflect information about such changes, these contributions are likely to be gradual modulations of the bulk density of states and difficult to distinguish and interpret in an experimental spectrum.

The preceding descriptions give a conceptual basis for classifying and discussing features of a single surface on a semi-infinite solid. While some of the theoretical

methods to be discussed use this geometry directly, many are based on a slab of finite thickness in the direction normal to the surface. In the limit of a thick slab, the front and back surfaces cannot interact, and quantities such as the surface charge distribution, surface density of states, etc. must converge to limits equal to the single-surface result. For any finite thickness, however, the states are classified differently, and their relation to states of the semi-infinite solid bears brief consideration.

Suppose we have a complete set of states for a semi-infinite solid, and form the slab by cutting off the surface region plus some number of bulk layers and joining this to its mirror image in the plane of the cut (which we chose to be a mirror plane of the bulk structure²). First consider the surface states. For a given \vec{k}_{\parallel} , we now have, to the first approximation, a degenerate pair of states at the previously found energy ϵ —one on each surface. However, the evanescent wave tail of each extends past the mirror plane, so in general there will be a nonzero matrix element of the Hamiltonian between the pair of states. The proper eigenstates of the slab will then be the even and odd linear combinations, and they will be split to energies $\epsilon \pm \delta$. Since the evanescent tails decay exponentially, the overlap and hence δ should decrease exponentially with slab thickness. This behavior with slab thickness constitutes a signature for identifying surface states in a slab calculation, as well as a means for extrapolating to the converged energy ϵ .

The above means of identifying surface states works well if the states are highly localized, which usually means that their energy ϵ is well away from band edges and implies that δ is small. For less well localized states near band edges, however, one of the pair $\epsilon \pm \delta$ may land within the band for any computationally practical slab. In this situation or one approaching it, the "two-by-two" formulation of the problem breaks down. While the surface state from the front surface is orthogonal to continuum states of that surface, its tail near the back surface will interact with continuum states near that surface, and the behavior of the surface-state derived pair of states with thickness will not display the simple asymptotic form discussed above. In this case, it may be difficult to determine whether or not a surface state will exist in the thick-slab limit by examining the spectra for several finite-thickness cases. In terms of physically relevant results, however, this is not an especially significant limitation, since a weakly bound surface state and a band-edge resonance will make comparable contributions to the surface density of states as previously discussed.

The more numerous states in a slab calculation are, of course, those related to the continuum states of the semi-infinite solid. Assuming a solution of this problem as before, suppose we choose a \vec{k}_{\parallel} and an E for which a single pair of propagating Bloch states exist. If we examine the states associated with each surface at the

mirror plane, it will in general not be possible to join them with continuous values and slopes. If the mirror plane is deep enough that the evanescent wave components have decayed to negligible values, we simply have a classic "particle in a box" quantization problem, and value and slope will match only at discrete energies. If the incident and reflected Bloch waves have equal magnitude wave vectors perpendicular to the surface, i.e., $k_z^{\pm} = \pm k_z$, a scattering phase shift can be defined in direct analogy with conventional scattering in one dimension. In this case, k_z will be quantized in units of $\pi/L(E)$, where L is an effective length that involves the actual thickness of the slab and the phase shift. Thus the eigenvalues of the slab could be found directly from the bulk $\epsilon(\vec{k})$ and the scattering phase shift of the surface in this case.

There are many more complex situations. The incident and reflected Bloch waves could have different $|k_z|$, there could be multiple reflected waves, or the energy could be near an extremum of an overlapping band so that long-range evanescent waves would have to be considered. Relations between single-surface and slab states have not been worked out for complex situations. Happily, they are not necessary to perform the calculations. By construction, the calculations always yield a spectrum of discrete energies and their corresponding wave functions for a given \vec{k}_{\parallel} . While the interpretation of these in terms of surface states, scattering resonances, and nonresonant scattering states often may not be possible, it is not necessary in the computation of, for example, the surface density of states. The slab thickness necessary to produce a given accuracy in the density of states can be judged directly from the level spacing.

In all the preceding discussion, nothing has been said about the surface region except that its potential is periodic parallel to the surface. What ultimately determines the surface region potential and, through it, the electron states, is the type of atoms in this region and their geometric arrangement. To conclude the discussion of general concepts, we will catalog the types of surface regions treated in the examples. First, one can have the ideal atomic geometry of the bulk continue right up to the vacuum. This is believed to be a good approximation for many metal surfaces, and has been verified in a limited number of cases by LEED intensity analysis. In this case, the potential differs from that of the bulk primarily outside the last atom plane, where the periodic parts of the potential fall to zero, and the average potential rises to the vacuum level, forming the so-called surface barrier. The distance scale for these changes is the order of the screening length. In the case of covalently bonded semiconductors (where the assumption of ideal atomic geometry is usually hypothetical) the existence of the surface barrier usually leads to one or more bands of surface states that lie at the upper end of the range of occupied states and are physically associated with broken bonds. Surface states have been found in calculations for undistorted metal surfaces, but, given the less directional nature of metallic bonding, their significance is not clear.

At the next level of complexity, the surface atoms can

²We have assumed for heuristic purposes that the solid possesses a mirror plane parallel to the surface of interest. In its absence the discussion needs to be generalized. See, for example, Appelbaum and Blount (1973).

be relaxed. This denotes motions that change the length and direction of the bonds between atoms in the first few layers, but do not change their periodic arrangement parallel to the surface. This is believed to occur on some metal and most semiconductor surfaces, although the latter are usually in the next category. There are two possible physical origins of surface relaxation. If interatom forces longer ranged than nearest-neighbor are important in the bulk lattice equilibrium, the balance of forces on the surface region atoms will be different and could move them. Secondly, atoms at the surface will form somewhat different chemical bonds than they do in the bulk because they will have some nonbonded electrons. The consequences of relaxation for the electronic structure are the possible existence of additional surface states and resonances not present for the unrelaxed surface, whose charge will be primarily localized in the disturbed bonds. This implies that the spectrum as measured by the local density of states around these bonds is different from the bulk density of states, which would certainly be expected. One could break the category of relaxed surfaces into two subcategories: relaxations that do not change the point group symmetry of the surface, and those that do. We are not aware of calculations involving the latter type of distortion, but it is easy to anticipate such consequences as additional critical points in surface-state bands and broadening of surface states at $\vec{k}_{||}$ points where they are crossed by bands of differing (bulk) symmetry.

The third category of surface region behavior is reconstruction. This denotes distortions that increase the size of the surface unit cell to some multiple of that of the ideal surface. Reconstruction patterns are designated in terms of the manner in which the ideal unit cell is multiplied in each of two directions with notations such as 2×1 , 7×7 , etc. The occurrence of reconstruction is easily detected by LEED and is common on semiconductor surfaces and rare on metals. In the presence of reconstruction, the larger unit cell must be used, implying a smaller surface Brillouin zone. The bulk band structure is folded into the new zone, so for a given $\vec{k}_{||}$ there will generally be more band extrema and less total gap space. Surface-state bands whose origin is not fundamentally related to the reconstruction may be split and may be broadened into resonances by mixing with bands that have been folded on top of them. New surface states and resonances may be formed by the bond distortions involved in the reconstruction.

The final category of surfaces is those with ordered chemisorbed layers. The layers may or may not increase the surface unit cell size, and the general discussions for the reconstructed or relaxed situations apply as appropriate. The adsorbed atoms or molecules form bonds to the substrate which are different from bulk bonds and therefore will give rise to additional bands of surface states and/or resonances. Of course, such features present on the clean surface from broken or modified bonds may be removed. States of the adsorbed species that do not participate in bonding to the substrate will nonetheless be described as surface states. They will acquire some bandwidth by indirect exchange of electrons through the substrate, and, of course, will be

narrow resonances instead of surface states where they overlap bulk bands.

II. *s*-*p* BONDED METALS

A. Jellium

Because of the weak interaction between the valence electrons and the ion cores in metals such as Na, K, or Al, they have served for many years as experimental prototypes of a highly useful theoretical construct—the electron gas (Pines, 1962; Kittel, 1963). In this model, the electrons are viewed as moving in a uniform neutralizing background of positive charge (referred to as jellium), interacting only among themselves. A single parameter characterizes the system—the electron density—defined by r_s , the radius of a sphere (in units of Bohr radii) containing one electron. By this measure, Na and Al are treated as electron gases with $r_s = 4$ and 2, respectively.

The surface of such an electron gas has been studied by assuming that the positive background terminates abruptly and calculating the response of the electron gas to this termination. Many such calculations have been made, by far the most complete and accurate of which are those of Lang (1969) and Lang and Kohn (1970, 1971). We review their results, which are also reviewed in detail by Lang (1973).

Lang and Kohn determine the response of the electron gas by solving Schrödinger's equation for the occupied levels of the semi-infinite system using an effective one-electron potential that depends on the electron density. The calculation is done self-consistently, so that the effective potential and the charge density it implies (via Schrödinger's equation) are mutually consistent.

The potential $V_T(z)$ is written as

$$V_T(z) = V_{es}(z) + V_{xc}(z), \quad (\text{II1})$$

where V_{es} is the electrostatic potential determined by Poisson's equation

$$\nabla^2 V_{es}(z) = -4\pi[(\rho_e(z) - \rho_0)\theta(-z)], \quad (\text{II2})$$

and V_{xc} is the effective exchange and correlation potential, written as a local function of the density,

$$V_{xc}(z) = F(\rho_e(z)). \quad (\text{II3})$$

The electron density is denoted by $\rho_e(z)$, the neutralizing positive background density by ρ_0 , and θ is the unit step function.

For the function F , Lang and Kohn used the Wigner interpolation form (Wigner, 1934)

$$F(y) = -y^{1/3} \left(0.984 + \frac{0.944 + 8.77y^{1/3}}{(1 + 12.57y^{1/3})^2} \right). \quad (\text{II4})$$

While the form of V_{xc} implied by (II3) and (II4) has substantial theoretical justification in the limit that $\rho_e(z)$ varies slowly as a function of z (Kohn and Sham, 1965), this condition is not satisfied at a surface. Its use in this region rests on empirical grounds. Equation (II4) has been applied with considerable success to bulk solids and atoms, and should work for surfaces. While we shall see that this expectation is substantially borne out, it is im-

portant to keep in mind that there are *a priori* limitations to a local density formalism. For example, it fails to properly go over asymptotically to the image potential, $1/4z$, in the vacuum region. No local approximation to exchange and correlation can accomplish this. Fortunately, this has only a small effect on the surface electronic properties, as demonstrated by Lang and Kohn, since so little electron density extends into the asymptotic region in which (II4) breaks down. Second, being a statistical theory, it works best for extended systems that interact strongly and for which many electronic states participate, and less well for isolated states.

Since the potential is one dimensional, the solution to Schrödinger's equation is comparatively straightforward. Self-consistency is basically achieved by an iterative process in which a potential is assumed and a charge density is calculated via Schrödinger's equation, and from that, with the use of (II1)–(II4), a new potential is calculated. This process is repeated until the input and output potentials agree to a prescribed amount.

Having summarized the basic physical assumptions that enter into the Lang and Kohn calculations, we turn to some of their results. In Figs. 1 and 2 we have plotted $\rho(z)$, $V_{es}(z)$, and $V_T(z)$ versus z (distance) for an $r_s = 4$ and 2 electron gas. The spatial origin is at the jellium discontinuity, with the positive background occupying the negative half-space. We are measuring distance in units of Fermi wavelength ($2\pi/k_F$), and energy in units of the Fermi energy. The zero of energy is fixed at the Fermi level. Focusing on the low-density case (Fig. 1), we see that the surface barrier arises primarily from V_{xc} , and that

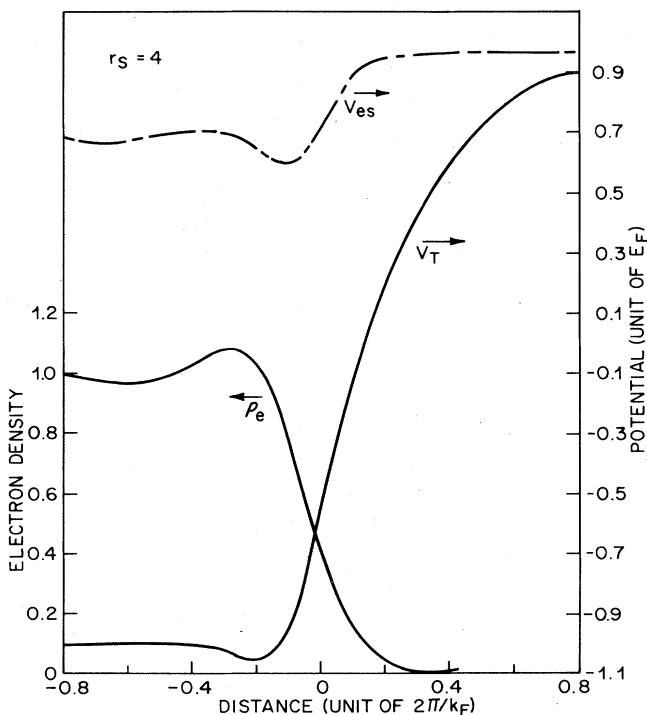


FIG. 1. Surface region electron charge density (ρ_e), electrostatic potential (V_{es}), and total potential (V_T) plotted versus distance normal to the surface for the jellium model of Na ($r_s = 4$). From Lang and Kohn (1970), with permission.

it is nearly twice the Fermi energy. The comparatively large size of V_T produces quantum or Friedel oscillations in the electron density, clearly visible in Fig. 1. These quantum oscillations have all but disappeared in the high-density limit (Fig. 2), a finding which is consistent with the fact that the surface barrier is only 30% larger than E_F . Once again V_T is dominated by V_{xc} , although not nearly so much as for $r_s = 4$. The work function, defined as $V_T(\infty) - E_F$, is 3.87 eV for $r_s = 2$ and 3.06 eV for $r_s = 4$. If one uses Al and Na as representative of $r_s = 2$ and 4, respectively, the calculated and experimentally measured work functions of polycrystalline samples agree to within 10%. This agreement is highly gratifying considering the relative simplicity of the jellium approximation.

While yielding excellent results for the work function, the surface energy calculated from the jellium model is not reliable. For higher densities, $r_s \lesssim 2.8$, the surface energy becomes negative, reflecting a well-known instability in bulk jellium (Herring, 1966). Clearly, it is desirable to include the discrete lattice in surface electronic calculations. For nearly free electron metals, jellium calculations can serve as a useful starting point. For example, from information about the linear response of a jellium surface to a uniform external electric field, Lang and Kohn were able to calculate to first order the change in work function produced by the discrete lattice. In addition, they showed that the introduction of a discrete lattice, assuming its effect on the valence charge density was small, allows one to recover positive surface energies in reasonable agreement with experiment for the nearly free electron metals. Jellium, however, clearly has its limitations. It fails, for example, to give spectral information about the surface and does not allow one to calculate the three-dimensional behavior of the electronic charge density.

We turn now to consider a number of computational schemes, developed during the last few years, in which

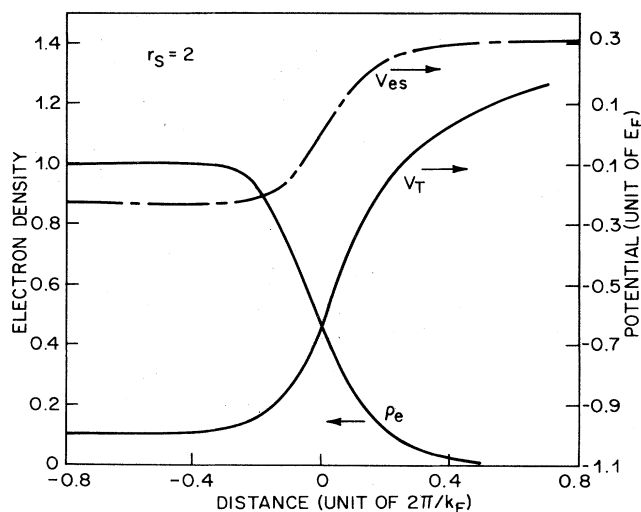


FIG. 2. Surface region electron charge density (ρ_e), electrostatic potential (V_{es}), and total potential (V_T) plotted versus distance normal to the surface for the jellium model of Al ($r_s = 2$). From Lang and Kohn (1970), with permission.

full account is taken of the three-dimensional nature of the surface.

B. Sodium

The first fully self-consistent calculation using a discrete lattice model was carried out by Appelbaum and Hamann (1972) for Na. In this calculation the surface is studied as the boundary of a semi-infinite solid. The potential has the form

$$V_T(\vec{x}) = V_{es}(\vec{x}) + V_{xc}(\vec{x}) + V_{ion}(\vec{x}), \tag{II5}$$

where V_{es} and V_{xc} are the electrostatic and exchange and correlation potentials, respectively, defined by (II2)–(II4). $V_{ion}(\vec{x})$ represents the nonelectrostatic electron-ion interactions.

The three-dimensional form of $V_T(\vec{x})$ complicates enormously the problem of solving Schrödinger's equation. To simplify this task as much as possible maximum use must be made of the two-dimensional translational symmetry possessed by the surface.

The potential $V_T(\vec{x})$ and wave function $\Psi_{k_{||}}^*(\vec{x})$ are expanded in a Laue representation (von Laue, 1931; Marcus and Jepsen, 1968),

$$V_T(\vec{x}) = \sum_{\vec{G}_{||}} \exp(i\vec{G}_{||} \cdot \vec{x}_{||}) v_{\vec{G}_{||}}(z), \tag{II6}$$

$$\Psi_{k_{||}}^*(\vec{x}) = \sum_{\vec{G}_{||}} \exp(i\vec{G}_{||} \cdot \vec{x}_{||} + i\vec{k}_{||} \cdot \vec{x}_{||}) u_{\vec{G}_{||}}(z). \tag{II7}$$

The coordinate system is oriented so that \hat{z} is normal to the surface, and $\vec{x}_{||}$ parallel to it. $\{\vec{G}_{||}\}$ is the set of reciprocal lattice vectors that characterizes the two-dimensional periodicity of the surface. Each wave function is labeled by a Bloch wave vector $\vec{k}_{||}$, which, together with the energy E , constitutes the basic quantum numbers of the problem. The Laue representation [(II6), (II7)] implies relatively rapid convergence of V_T in a plane wave basis. To achieve this one must use for V_{ion} a model or pseudopotential in which the strong atomic core potential has been effectively removed.

Substituting (II6) and (II7) into Schrödinger's equation results in a set of coupled differential equations for $u_{\vec{G}_{||}}(z)$, viz.,

$$\left[-\frac{1}{2} \frac{d^2}{dz^2} + \frac{1}{2} (\vec{k}_{||} + \vec{G}_{||})^2 - E \right] u_{\vec{G}_{||}}(z) + \sum_{\{\vec{G}'_{||}\}} v_{\vec{G}'_{||}}(z) u_{\vec{G}'_{||}}(z) = 0, \tag{II8}$$

where the number of $\vec{G}'_{||}$'s retained is determined by the strength of V_T .

For a given E and $\vec{k}_{||}$, (II8) can be integrated numerically assuming $u_{\vec{G}_{||}}(z)$ and $(d/dz)u_{\vec{G}_{||}}(z)$ are specified on a plane, say $z = z_1$. Integration to another plane $z = z_2$ is represented concisely by defining a transfer matrix $\vec{T}_{2,1}$,

$$\vec{u}_2 = \vec{T}_{2,1} \vec{u}_1, \tag{II9}$$

where \vec{u}_i is a vector constructed from $u_{\vec{G}_{||}}(z_i)$ and $du_{\vec{G}_{||}}(z_i)/dz$,

$$\vec{u}_i = \begin{pmatrix} u_{\vec{G}_1}(z_i) \\ \vdots \\ u_{\vec{G}_N}(z_i) \\ (d/dz)u_{\vec{G}_1}(z_i) \\ \vdots \\ (d/dz)u_{\vec{G}_N}(z_i) \end{pmatrix}. \tag{II10}$$

Knowledge of $\vec{T}_{2,1}$ constitutes only a partial solution to the problem; satisfying the appropriate boundary conditions on $\vec{u}(z)$ for z in the bulk and in the vacuum represents the remainder. The boundary value problem is illustrated in Fig. 3, where space is divided into three regions by two planes parallel to the surface. To the left of the bulk plane V_T is assumed equal to its infinite bulk solid value, and to the right of the vacuum plane V_T is assumed to have no spatial variation parallel to the surface. In both these regions the solutions \vec{u}_i to the Schrödinger equation are known. In region I they are Bloch waves that either propagate or decay to the left, and in the region III they have the form $\exp[i(\vec{k}_{||} + \vec{G}_{||}) \cdot \vec{x}_{||}] \varphi_{\vec{G}_{||}}(z)$, where $\varphi_{\vec{G}_{||}}(z)$ decays exponentially with increasing z . Connecting the solutions of known form in region I to region III is the job of the transfer matrix. The boundary conditions can be written as

$$\vec{u}_b = \vec{T}_{b,v} \vec{u}_v, \tag{II11}$$

where \vec{u}_v and \vec{u}_b are sums of allowed vacuum and bulk solutions, respectively, for the given E and $\vec{k}_{||}$.

For E within a bulk band, \vec{u}_b is assumed to contain an incident propagating wave of unit amplitude and (II11) then uniquely specifies the remainder of \vec{u}_b and \vec{u}_v , and through (II9), \vec{u} everywhere. For E in a bandgap no propagating Bloch waves exist, only evanescent waves, and (II11) can have solutions only at special energies

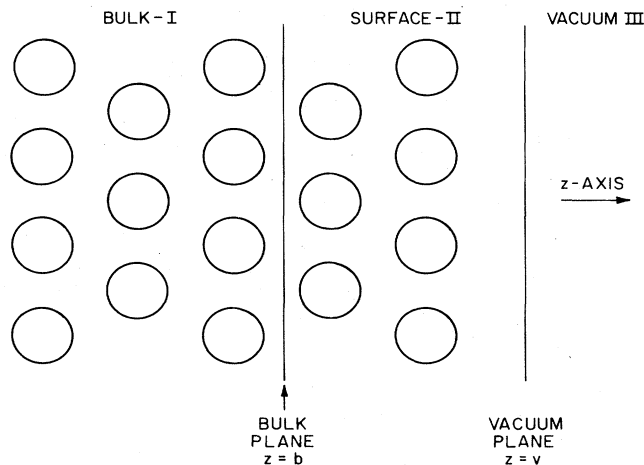


FIG. 3. Schematic representation of the three regions into which space is divided in the method developed by the authors. In region I the disturbance in the potential produced by the surface is assumed to have been screened to negligible values. In region II, only the nuclear coordinates are specified and the potential is allowed to adjust itself self-consistently. In region III, the variation of the potential parallel to the surface is assumed negligible.

$E_n(\vec{k}_\parallel)$, which define the spectral location of the surface states. These states, free to propagate along the surface, are bound to the surface region by the vacuum barrier on one side and the bandgap of solid on the other. Their energies are found by varying E in a bandgap and searching for possible zeros of the multidimensional vector $\vec{u}_b - \vec{T}_b \vec{u}_v$. It must be borne in mind that \vec{k}_\parallel is always fixed, and that a bandgap for a fixed \vec{k}_\parallel can and does often coincide with regions of allowed electron state density at other \vec{k}_\parallel 's.

Having outlined the method, we consider its application to Na(100). The surface has no occupied surface states, so only band states are needed for self-consistency. For V_{ion} , the Ashcroft model potential (Ashcroft, 1966) was used and the bulk matching plane was placed between the second and third layer. Placing it between the third and fourth layer caused only very small changes in any of the results. The work function calculated for Na is shifted by 0.3 eV downward from that of jellium because of the inclusion of the discrete lattice. This shift is consistent with that calculated by LK from perturbation theory and is in closer agreement with experiment than is jellium. The Friedel surface oscillations and the bulk charge density oscillations appear to superpose linearly—not surprising considering that both represent 10% effects.

The three-dimensional potential along rays normal to the surface is plotted in Fig. 4. The potential is still far from uniform 2 Å outside the last plane of Na, where there remains a 0.4 eV variation parallel to the surface.

C. Lithium

An alternative geometrical approach that is frequently adopted in studying solid surfaces is the slab geometry. The first self-consistent calculation using this geometry was that of Alldredge and Kleinman (1974). The electron potential is treated as in (II5), except the added flexibility of having a nonlocal ion-electron potential is allowed.

Schrödinger's equation is solved by the following device. The slab of material studied is embedded in a larger one-dimensional channel of width L whose infinite

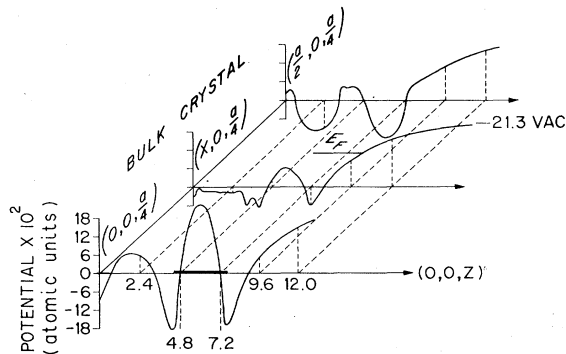


FIG. 4. Potential at the Na(100) surface along three lines normal to the surface. The bottom line goes through a surface atom (heavy bar), and the top line passes through the midpoint between nearest-neighbor surface atoms. Distance is in atomic units. From Appelbaum and Hamann (1972).

potential walls are placed a few lattice spacings from the last physical atomic plane, so that their effect on the real surface barrier is minimized. The wave function $\Psi_{\vec{k}_\parallel}(\vec{x})$ is expanded in a basis set $\{\Phi_{\vec{G}_\parallel, k_n}(\vec{x})\}$ defined by

$$\varphi_{\vec{G}_\parallel, k_n}^{\vec{k}_\parallel}(\vec{x}) = \exp(i\vec{G}_\parallel \cdot \vec{x}_\parallel + i\vec{k}_\parallel \cdot \vec{x}_\parallel) \sin(k_n z + n\pi/2), \quad (\text{III2})$$

where

$$k_n = n\pi/L, \quad n = 1, 2, \dots \quad (\text{III3})$$

The diagonalization of the Hamiltonian matrix yields a discrete spectrum of allowed energies for any \vec{k}_\parallel . As the slab is allowed to grow in size, the spacing between most levels diminishes accordingly, and in the limit of an infinitely thick slab, goes over to a continuum of allowed $E_{\vec{k}_\parallel}$, forming energy bands. Those levels that remain isolated from the banding levels are surface states. They always occur in pairs, and they are spatially localized.

The strength of the slab geometry is that all states, continuum and surface, are discrete and are treated in the same way. Its weakness lies in the fact that the computational effort involved grows as a high power of the number of layers. This forces one to work with comparatively thin slabs, and size and surface effects can become entangled. We now turn to the specific calculation; Alldredge and Kleinman studied the Li(100) surface using 13 atomic layers which allowed them to exploit the mirror symmetry possessed by the slab. A nonlocal pseudopotential was chosen of the form

$$v_{\text{ps}}(\vec{r}, \vec{r}') = v(\vec{r})\delta(\vec{r} - \vec{r}') + E_{\text{rep}}\varphi_{1s}(\vec{r})\varphi_{1s}(\vec{r}'), \quad (\text{III4})$$

where $v(\vec{r})$ is the atomic potential, E_{rep} , empirically adjusted, equals 4.4884 Ry, and φ_{1s} is the 1s wave function calculated from Herman and Skillman (1963). This choice, unfortunately, was not optimum with respect to the Li band structure, and as a consequence, the calculated work function for Li(100) was 3.71 eV, almost 1 eV greater than experiment. The charge density calculated is shown in Fig. 5 along lines normal to the surface and through surface atoms at (0, 0), second layer atoms at $(\frac{1}{2}, \frac{1}{2})$ and various interstitial regions. The prominence of the first Friedel peak is very clear in almost all lines. Alldredge and Kleinman (1974b, c) also calculated the force on the first few atomic layers adjacent to vacuum. They found sizable inward forces on the first Li plane which they attributed to a tendency of the surface layer to contract under the electrostatic force of the first Friedel peak.

D. Aluminum

Chelikowsky *et al.* (1975) have taken a somewhat different approach in treating the slab geometry. During the course of their study of Al(111), they, following Cohen *et al.* (1975), embedded a 12-layer Al slab in an empty tetragonal periodic lattice. This empty lattice has the same periodicity parallel to the slab surfaces as that of the Al slab; normal to the surface the lattice has an 18-layer repeat distance, which allows a vacuum region of ~ 4 Å per surface.

With periodic boundary conditions the natural basis for expanding the eigenvectors becomes

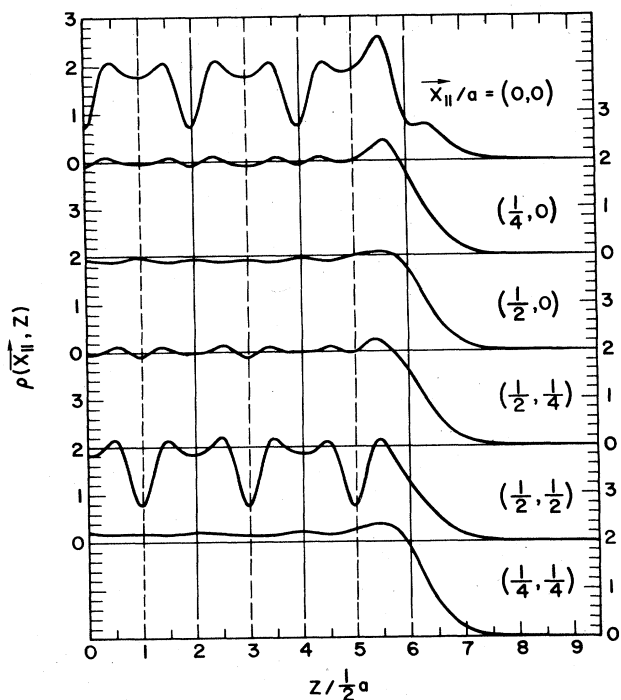


FIG. 5. Valence charge density for the Li(100) surface plotted along several lines normal to the surface. (0,0) passes through a surface atom and (1/2, 1/2) through a second layer atom. Distance and charge are in lattice constant units, $a/2$ and ea^{-3} , respectively. From Allredge and Kleinman (1974a), with permission.

$$u_{\vec{G}_{||,n}}^{\vec{k}_{||}}(\vec{x}) = \exp(i\vec{G}_{||} \cdot \vec{x}_{||} + i\vec{k}_{||} \cdot \vec{x}_{||} + ik_n z), \quad (\text{III15})$$

where

$$k_n = 2\pi n/L, \quad n = 0, \pm 1, \dots$$

and L is the length (normal to the surface studied) of the tetragonal unit cell. A sufficiently large number of $u_{\vec{G}_{||,n}}^{\vec{k}_{||}}(\vec{x})$ are retained for convergence, with Löwdin perturbation techniques used to simplify the matrix diagonalization (Löwdin, 1951). The calculation is carried to convergence using the core potential for Al^{3+} proposed by Animalu and Heine (1965). The extracted work function is 5.16 eV, considerably larger than experiment. Aluminum has a number of long-range surface states below the Fermi energy and one such state is shown in Fig. 6. This state, which is comparatively localized compared to others that exist on this surface, extends quite deeply into the bulk. Chelikowsky *et al.* found considerable Friedel oscillation in their charge density, as well as important modifications in the surface barrier in the first two atomic layers. This result is quite interesting considering that Lang and Kohn (1970, 1971) found almost no Friedel oscillations present for $r_s \approx 2$, which would be appropriate to Al.

III. SEMICONDUCTORS

A. Si(111)1 × 1

Large numbers of calculations have been made for this surface. We shall review three, from Appelbaum and

Hamann (1973, 1974), Pandey and Phillips (1974a, b; 1976), and Schlüter *et al.* (1975), as representative of the state of the art.

This surface occurs in three structural forms, a metastable 2×1 , a stable 7×7 , and a high-temperature 1×1 . The calculations we review in this section are for the 1×1 form. They allow, however, for normal displacements of the outermost surface plane.

The methods used by Appelbaum and Hamann have already been reviewed in Sec. II.B. We summarize their results. The ionization potential (I.P.), which denotes the distance between vacuum level and valence band maximum, is calculated to be 5.3 eV—in very good agreement with data for the stable 7×7 surface (within 0.2 eV). (There are no measurements of the 1×1 form.) The I.P. is found to be insensitive to small normal displacements. For all geometries a “dangling bond” surface-state band exists that is highly localized in front of and just behind the surface atoms. A plot of the charge density in an occupied state in this band is shown in Fig. 7. This band is only partially occupied and, lying as it does within the gap between the valence and conduction bands, defines a surface Fermi level, E_{FS} . For 0.34 Å inward displacement of the surface plane, E_{FS} lies 0.3 eV above the valence band maximum, in close agreement with Si(111) 7×7 experimental data. For relaxation inward, additional bands of surface states occur at the bottom of the lowest valence band and within the p -like region of the bulk band structure. The latter has charge localized on the bonds between the first and second atomic layers and is shown in Fig. 8.

These surface-state bands, among or below the valence bands, had not been predicted before Appelbaum and Hamann (1974). Experimental evidence for their existence can be found in both photoemission and electron energy loss scattering. The more recent work of Schlüter *et al.* (1975), using the slab geometry (described in Sec. II.D), confirm these spectral findings. They obtain an ionization potential of ~ 4.0 eV, but remark that their methods are presently unsuitable for extracting the correct asymptotic vacuum level because

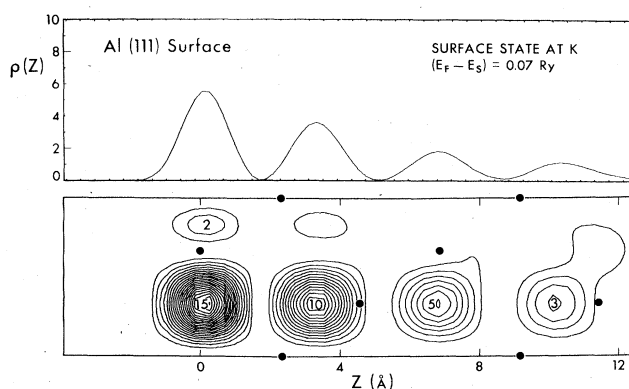


FIG. 6. Surface state at the Al(111) surface. The upper portion shows the planar average charge density as a function of normal coordinate (the surface is here to the left), and the lower portion shows contours of constant charge density in a (110) plane, with atom centers indicated by heavy dots. From Chelikowsky *et al.* (1975), with permission.

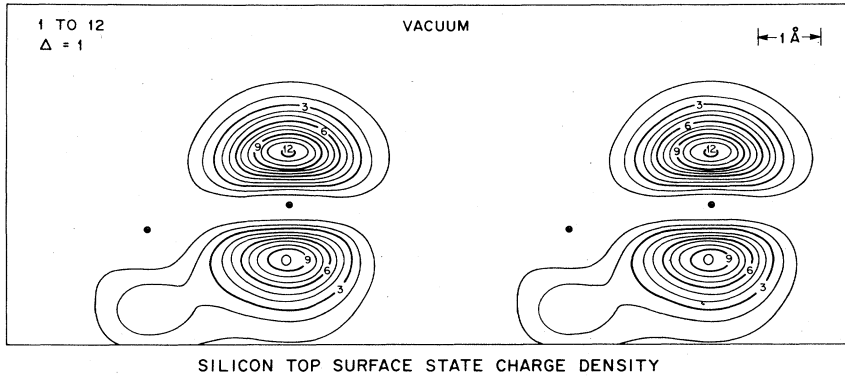


FIG. 7. Contours of constant charge density for the occupied portion of the dangling bond surface state on the Si(111) surface. The energy of this state is within the absolute gap. Dots locate atom centers, the vacuum is above, and charge density is in a.u. $\times 10^3$. From J. A. Appelbaum and D. R. Hamann, in *Proceedings of the Twelfth International Conference on the Physics of Semiconductors*, edited by M. H. Pilkuhn (Teubner, Stuttgart, 1974), p. 675.

of the proximity of the slabs to each other in their periodic slab formulation.

The methods of Pandey and Phillips are quite different from the above. They have invigorated the empirical tight-binding approach to calculating bulk spectra (Dresselhaus and Dresselhaus, 1967) and surface spectra (Hirabayashi, 1969). This method has a long and venerable history in chemistry, but has been viewed with considerable reservation when applied to semiconductors because of its apparent failure to satisfactorily reproduce their band structure. The method, in the form applied by Pandey and Phillips, assumes that the wave functions of a thin slab can be written as

$$\varphi_{\vec{k}_\parallel} = \sum_{j,m} \exp(i\vec{k}_\parallel \cdot \vec{R}_m) a_{\vec{k}_\parallel}^{j,m} \psi_j(\vec{r} - \vec{R}_m), \quad (\text{III1})$$

where \vec{k}_\parallel is the surface Bloch wave vector, and $\psi_j(\vec{r} - \vec{R}_m)$ is an orthogonalized atomic orbital of either s or p symmetry about atomic site \vec{R}_m . Using (III1) as a basis, seven parameters characterize the matrix elements of the Hamiltonian. They are the diagonal s - p energy splitting (1 parameter), the s and p nearest-neighbor matrix elements (4 parameters), and the pp second-neighbor matrix elements (2 parameters). These parameters are determined by calculating the mean-squared error between tight-binding and pseudopotential energy levels for bulk Si at many points in the zone for the valence and lowest conduction bands, and varying the parameters to find the absolute minimum. This highly overdetermined fit yields satisfactory band structure over the entire range of interest. Pandey and Phil-

lips postulate no change in these parameters at the surface of the slab (assuming no relaxation) and calculate the spectrum of a 20-layer Si slab oriented with respect to the (111) surface. Excellent correspondence with Appelbaum and Hamann's spectra at symmetry points is obtained. To incorporate relaxation, they make the ansatz that the matrix elements $M_{jk}(\vec{R}_m)$ between nearest neighbor orbitals $\psi_j(\vec{r})$ and $\psi_k(\vec{r} - \vec{R}_m)$ depends on \vec{R}_m through a Hückel relationship,

$$M_{jk}(\vec{R}_m) = M_{jk}(\vec{R}_m^0) \exp[\beta(|\vec{R}_m^0| - |\vec{R}_m|)], \quad (\text{III2})$$

where β is an empirical "overlap" parameter used for all jk and \vec{R}_m^0 is the separation of orbitals j, k before relaxation. The parameter β was fixed by fitting the calculated surface spectra to the calculations of Appelbaum and Hamann (1974, 1975). Once again good agreement with the spectra was obtained with a single parameter for all orbitals. The density of states on the surface layer, four layers into the slab, and in the bulk, calculated by Pandey and Phillips, is shown in Fig. 9. Notice the prominent position of the dangling bond states in the first layer and the location of critical points due to the back bond and bottom of the band surface states caused by the relaxation. These features are the ones observed in photoemission on Si(111) 7×7 .

B. Si(111) 2×1

The Si(111) surface occurs in a metastable 2×1 form when prepared by cleavage. This surface has been the subject of a large number of theoretical calculations. Two of the most realistic are those of Schlüter *et al.*

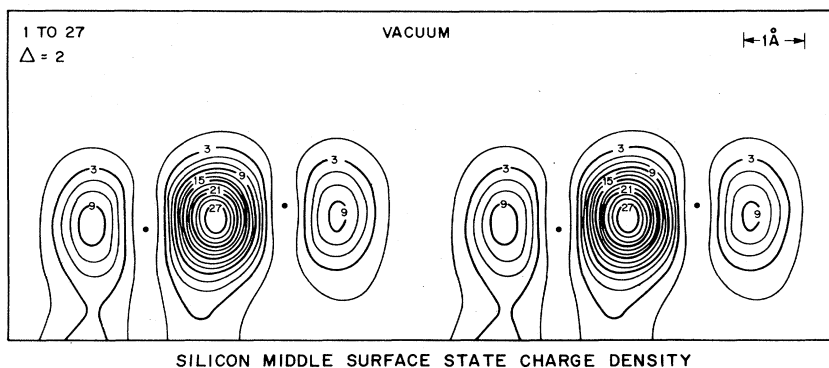


FIG. 8. Contours of constant charge density for the Si(111) back bond surface-state band lying in internal gaps, 2 to 3.5 eV below the valence band maximum. This state occurs only for a substantial degree of inward relaxation of the surface layer, 0.34 Å in this case. Charge density is in a.u. $\times 10^3$, and dots locate atom centers. From J. A. Appelbaum and D. R. Hamann, in *Proceedings of the Twelfth International Conference on the Physics of Semiconductors*, edited by M. H. Pilkuhn (B. G. Teubner, Stuttgart, 1974), p. 675.

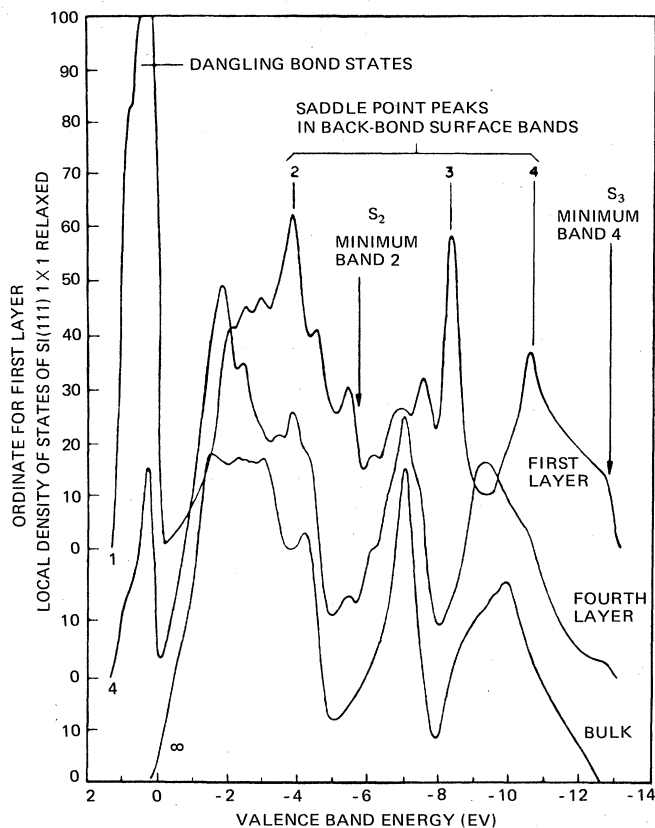


FIG. 9. Density of states for the Si(111) surface atom layer, for the fourth layer in from the surface, and for the bulk. Relaxation of 0.34 Å is assumed, and spectral features arising from the dangling bond and from relaxation induced surface states are identified. From Pandey and Phillips (1976), with permission.

(1975) and Pandey and Phillips (1975). Schlüter *et al.* performed a self-consistent calculation assuming the geometry used by Haneman (1961). In this geometry alternating rows of atoms are raised and lowered by 0.18 and 0.11 Å, respectively, and second layer atoms are shifted laterally to preserve the length of the back bonds. The main emphasis was on studying gap surface states. The dangling bond band is split by the reconstruction, the states associated with the expanded atoms dropping in energy and those associated with the relaxed atoms forming the higher energy branch. Their density of states is plotted in Fig. 10. The charge density on the two bands of states is shown in Fig. 11(a) and 11(b).

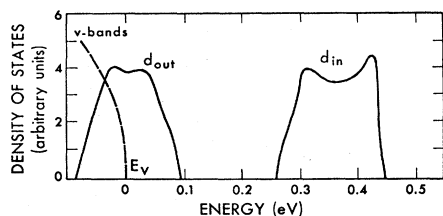


FIG. 10. Density of states for the split dangling bond surface-state band on the 2x1 reconstructed Si(111) surface. From Schlüter *et al.* (1975), with permission.

Notice that these states have little overlap. Infrared absorption was measured on the 2x1 surface by Chiaraotti *et al.* (1971). It begins at ~0.3 eV and peaks at ~0.5 eV. Theoretical calculations predict similar behavior, although both threshold and the peak are shifted to lower energy by ~0.1 eV. This surface is predicted to be ionic, with charge flowing from the lowered atoms to the raised ones, a finding which is consistent with slow electron-surface phonon interactions observed by Ibach (1971).

Pandey and Phillips (1975) have also studied this surface using empirical tight-binding calculations and allowing for bond length changes by means of Eq. (III2). They explored a large number of different geometric configurations and concluded that bond length modifications were necessary to account for experimentally measured spectral features on this surface. Their geometric model has vertical displacements of alternating rows of

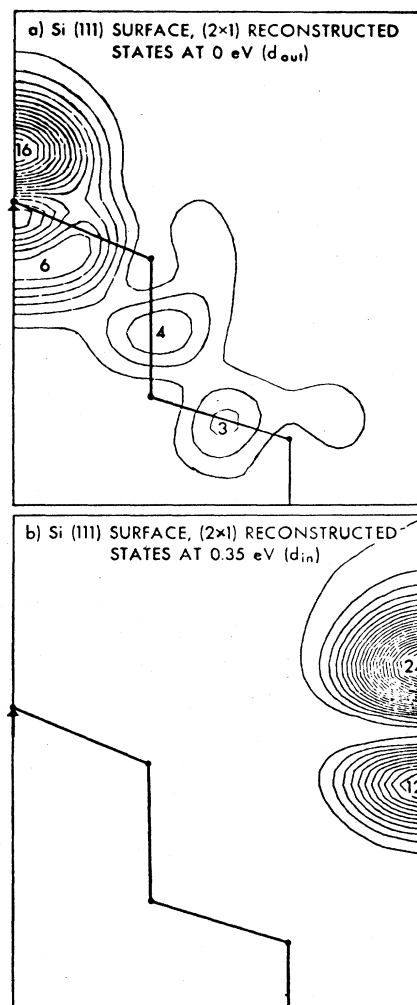


FIG. 11. Contours of constant charge density for the low-energy (top) and high-energy (bottom) portions of the split dangling bond surface-state band on the 2x1 reconstructed Si(111) surface. Inward and outward motions of surface atoms from the ideal lattice position are indicated by arrows. Dots indicate atom centers, and lines indicate bonds. From Schlüter *et al.* (1975), with permission.

surface atoms by 0.29 Å (inward) and 0.35 Å (outward), with 0.24 Å uniform displacement of the second layer. These displacements split the gap surface-state band as discussed above, producing an indirect threshold of 0.33 eV and a direct threshold of 0.65 eV. They invoke excitonic effects to account for the experimental absorption peak at 0.45 eV. They emphasize that the postulated displacements also account for angular photoemission data showing a peak at ~ 1.2 eV—referenced to the valence band maximum (VBM)—which has threefold symmetry and which is caused by back bond stretching. Similar conclusions were drawn by Appelbaum and Hamann (1975a) from calculations of 1×1 surfaces that were allowed to have expanded and contracted outermost atomic planes, without invoking second layer motions.

C. Si(100) 2×1

Extensive calculations have been carried out for the Si(100) surface by Appelbaum, Baraff, and Hamann (1975a, b, c). The unreconstructed form of this surface, viewed from above, is shown in Fig. 12. Two bonds per surface atom are broken on this surface, leaving the surface in a chemically unstable state, which is relieved by surface reconstruction. The arrangement of atoms within the 2×1 reconstructed unit cell is not known from LEED studies, but two chemically plausible models have been suggested for this reconstruction. The first involves surface pairing or dimerization in order to re-bond the broken bonds (Schlier and Farnsworth, 1959). The second removes alternate rows of surface atoms and postulates that the remainder strengthen their bonds to the substrate forming two double bonds (Phillips, 1973). Self-consistent calculations performed for both models, using the methods of Appelbaum and Hamann, clearly favor the dimer model. The most telling evidence is contained in a comparison of the density of states in the surface region calculated theoretically for both models with ultraviolet photoemission spectra taken by Rowe and Ibach (1974). Such a comparison is

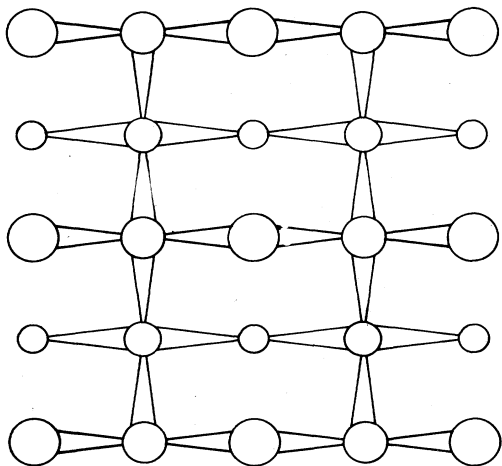


FIG. 12. Unreconstructed Si(100) surface geometry, showing the first four atom layers and their bonds viewed from above. The largest circles are first layer, the next smaller second layer, etc. From Appelbaum *et al.* (1975a).

made in Fig. 13. The curves are aligned for equal thresholds and the dimer model clearly is favored over the vacancy model. The peak at -2.5 eV, a distinctive signature of this surface, is caused by the p -portion of the dimer bond. It shows up so sharply because hybridization between it and other bonds is suppressed due to the misalignment of the dimer relative to all other bulk bonds. The higher energy shoulder is caused by the bent back bonds, which push spectral weight (in the form of a surface-state band) above portions of the p bands, and a π -bond-like state, derived from broken bonds of the ideal surface, which pulls spectral weight down from the absolute gap. The spectral features below -9 eV are not seen clearly in photoemission. This is believed to be caused by matrix element effects, which suppress the s portion of the spectrum relative to the p .

The surface Fermi level was calculated to lie at the VBM, in accord with experiment (Rowe, 1974) and in contrast with the vacancy model which has its Fermi level centered in the bandgap. The total charge density for the dimer model is shown in Fig. 14. Notice that the dimer bond, geometrically at a single bond distance, is remarkably like bulk bonds. The spectrum of this surface achieves its characteristic shape because of orientational effects rather than because the dimer bond is particularly different from a bulk bond.

D. Polar semiconductors

There have been a number of tight-binding calculations (Joannopoulos and Cohen, 1974; Calandra and Santoro, 1975) and abrupt junction calculations (Garcia, 1975) published of the electronic spectrum of compound semiconductor surfaces. In addition, self-consistent calcu-

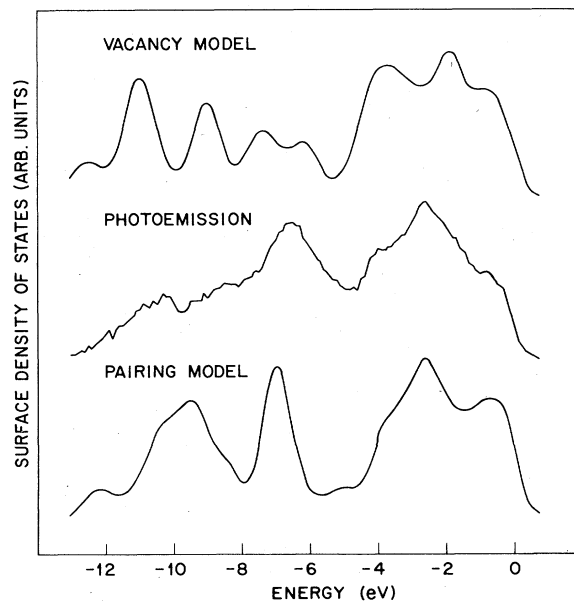


FIG. 13. Density of states of the first two atom layers for the 2×1 reconstructed Si(100) surface computed using two different models for the surface geometry. uv photoemission data at $\hbar\omega = 21.2$ eV from Rowe (1974) is shown with a smooth secondary background subtracted. From Appelbaum *et al.* (1975b).

lations for the GaAs(100) (Appelbaum, Baraff, and Hamann, 1976) and GaAs and ZnSe(110) (Chelikowsky and Cohen, 1976) surfaces have just become available. We concentrate on the results from the self-consistent calculations. For GaAs(110), two bands of gap surface states separated by 1.5 eV exist and are associated with the Ga and As atoms, respectively. With the As surface band full and the Ga band empty, this splitting widens considerably in going to ZnSe. The tight-binding and abrupt junction results are in qualitative agreement with these results. For the Ga terminated surface of GaAs(100), two bands of gap surface states were found corresponding to the two broken bonds present on this surface. One was dangling-bond-like and $\frac{3}{4}$ occupied, and the other empty and lying within the surface atom plane along the broken bond direction. Contour plots of these states are seen in Figs. 15 and 16. For both (110) and (100) surfaces it was concluded that the effective ionic character of the atoms at the surface appeared similar to that in the bulk, in one case from the shape of the charge density contours, in another [GaAs(100)] from a direct calculation of the effective charge on the Ga surface atoms. This was done in a completely unambiguous fashion by studying the change in surface dipole potential as a function of the displacement of the last atom plane. The efficient screening of the surface atoms, which appears to leave them in a bulklike charge state, helps explain the qualitative similarity of the more accurate of the tight-binding calculations with experiment.

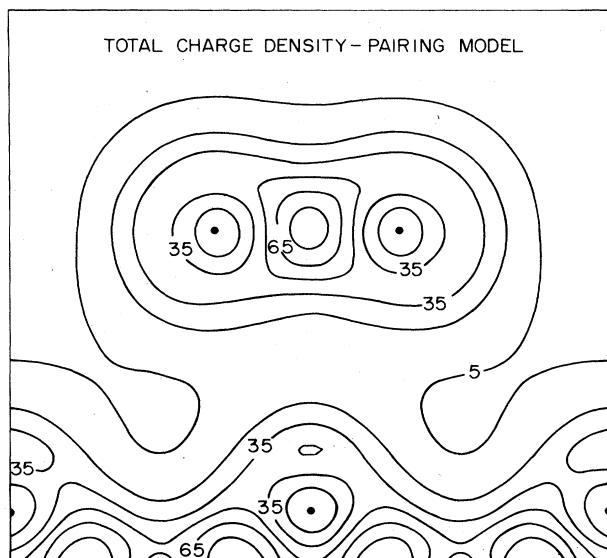


FIG. 14. Contours of constant charge density for the total charge of the pairing model for the 2×1 reconstructed Si(100) surface. The dimer bond between the paired first layer atoms is seen to be similar in shape to the partially visible bulk bonds between the fourth and fifth layers. Second and third layer atoms are out of the plane of the plot. From Appelbaum *et al.*, Phys. Rev. Lett. 34, 806 (1975).

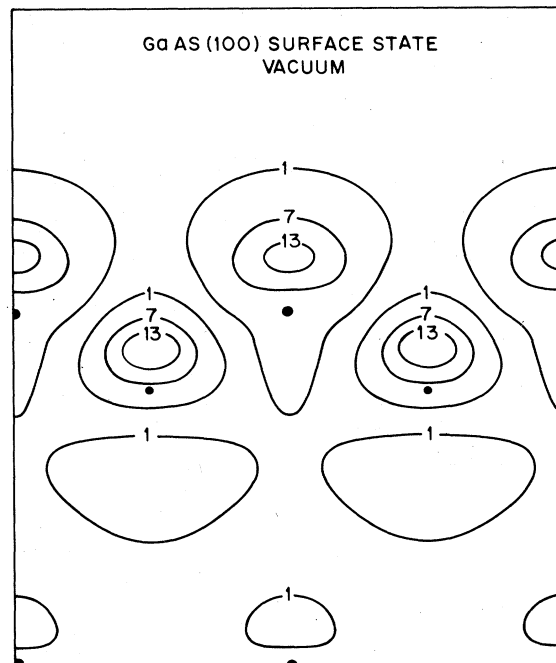


FIG. 15. The dangling bond electron density at $\vec{k}_{\parallel} = J'$ is contour plotted on a plane normal to the (100) surface and passing through the back bond between the surface Ga atoms (shown as heavy dots) and their second layer As atoms (shown as light dots). The density is in a.u. $\times 10^3$. From Appelbaum *et al.* (1976).

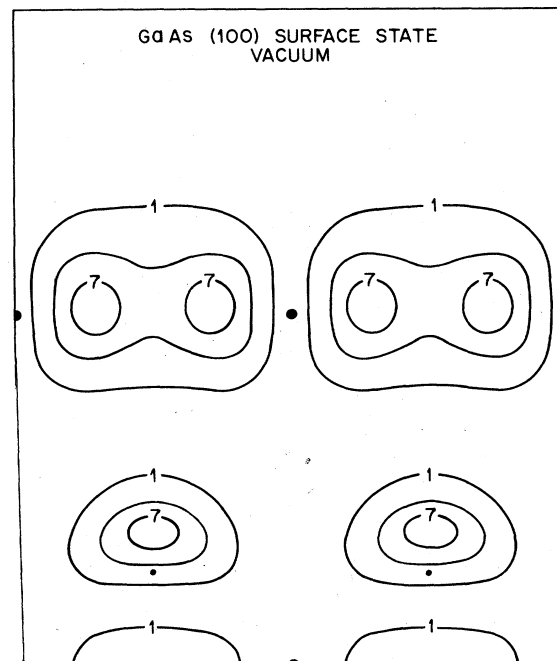


FIG. 16. The bridge bond electron density at $\vec{k}_{\parallel} = J'$ is contour plotted on a plane normal to the (100) surface and oriented in the direction of the surface broken bonds. The Ga(As) atoms are shown as heavy (light) dots and the density is in a.u. $\times 10^3$. From Appelbaum *et al.* (1976).

IV. TRANSITION METALS

A. Cu

Forstmann and Heine (1970) and Forstmann and Pendry (1970) studied the existence of surface states on Cu(100). Their model, extensively used by Heine (1962) and Jones (1968) for semiconductors, assumes a semi-infinite geometry in which the bulk potential continues undisturbed up to the first symmetry plane beyond the surface atoms, at which point it changes discontinuously to a constant value determined by the experimental work function. Emphasis is placed on surface states, and Schrödinger's equation is solved for energies E within a bandgap by solving for the evanescent Bloch waves of the periodic crystal and matching them to exponentially decaying waves in the constant potential vacuum region. This procedure is most likely to be adequate for weakly bound surface states, where the precise form of the surface potential may not be of paramount importance. They treat the bulk Bloch functions by an empirical adaptation of the KKR method (Korringa, 1947; Kohn and Rostoker, 1954), in which the Cu muffin-tin potential is assumed to scatter only d waves, with a phase shift parametrized as a simple resonance form.

The surface state Forstmann and co-workers studied was in a hybridization gap between sp and d -like bands. A surface state was found split ~ 0.3 eV from the lower portion of the gap (only $\vec{k}_\parallel = 0$ is studied). This relatively weak splitting suggests a comparatively delocalized state, although the spatial nature of the state was not studied. They argue that this kind of hybridization gap surface state is of the type seen in photoemission measurements on Ni and Cu (Callcott and MacRae, 1969). For this to be the case, one would expect that the state would have to be comparatively well localized in the surface region. The resolution of this question will have to await more extensive theoretical work.

B. W and Mo

The study of surface states on W and Mo by Kasowski (1975) treats the surface within a slab geometry and uses a comparatively new method for solving Schrödinger's equation—the linear combination of muffin-tin orbitals (LCMTO) technique due to Andersen and Kasowski (1971). The non-self-consistent potential used is constructed by taking a superposition of overlapping atomic charge densities to represent the charge within the slab and using Slater exchange and Poisson's equation to calculate a potential from it. The angular dependence of the potential within each atom cell is expanded in spherical harmonics. The LCMTO method is patterned after the traditional linear combination of atomic orbitals (LCAO) method, but in place of atomic orbitals it uses orbitals which allow analytic reduction of all the multicentered integrals to a relatively small number of radial integrals. These multicentered integrals are usually the bane of LCAO calculations. The special orbitals (MTO) used in the LCMTO method are defined as follows. A sphere of radius A , around each atomic site \vec{R}_i , is introduced and a spherically averaged potential calculated. The solution of Schrödinger's equation

for an energy $E < 0$ (vacuum level) within the sphere is denoted by $\omega_l(r)$, where l labels the angular momentum state involved.

The MTO about site \vec{R}_i is then defined as

$$\varphi_{ilm}(\vec{x} - \vec{R}_i) = Y_{lm}(\vec{x} - \vec{R}_i / |\vec{x} - \vec{R}_i|) \times \begin{cases} w_l(|\vec{x} - \vec{R}_i|) + a_l j_l(\kappa |\vec{x} - \vec{R}_i|), & |\vec{x} - \vec{R}_i| < A_i, \\ b_l n_l(\kappa |\vec{x} - \vec{R}_i|), & |\vec{x} - \vec{R}_i| > A_i, \end{cases} \quad (\text{IV1})$$

where j_l and n_l are spherical Bessel and Neumann functions and a_l and b_l are coefficients fixed by continuity requirements on φ_j and its derivative across the sphere. The energy $\kappa^2 < 0$ determines the rate of decay of the orbital tails and is treated as a variational parameter.

A wave function with wave vector \vec{k}_\parallel is then written as

$$\Psi_{\vec{k}_\parallel}(\vec{x}) = \sum_{j,i} c_{ji} \sum_m \exp(i\vec{k}_\parallel \cdot \vec{R}_{jm}) \varphi_{j,i}(\vec{x} - \vec{R}_{jm}), \quad (\text{IV2})$$

where j labels a particular atomic layer, m the atom in that layer, and i a particular MTO. The c_{ji} are determined by minimizing the energy in the usual manner. Note that while a muffin-tin potential is introduced for use in defining the orbitals, the complete non-muffin-tin potential is used in calculating the Hamiltonian matrix.

A 20-layer slab was used by Kasowski in his study of W and Mo(100) surfaces. In contrast to the situation on Cu and Ni, he finds surface states on W and Mo that are strongly localized within the outermost two or three atomic layers. These states are sensitive to assumptions concerning surface relaxation both with respect to spatial extent and with respect to their position in energy. The state studied in W(100) lies at -0.22 Ry (relative to the Fermi level) and shifts to -0.14 with a 3.2% decrease in the first to second layer back bond distance. For Mo a 3% bond length decrease is required to induce a surface state at -0.05 Ry. A full study of the spectrum has not been undertaken for these systems and the importance of self-consistency has not yet been explored.

C. Fe(100)

Caruthers and Kleinman (1975) have studied the energy spectrum of a 13-layer Fe slab. The method used is basically that of Alldredge and Kleinman (1974) with the plane wave basis (III2), supplemented with localized d functions, $\varphi(\vec{r} - \vec{R}_n)$ that are defined by

$$\varphi(\vec{x} - \vec{R}) = Y_{2m}(\vec{x} - \vec{R} / |\vec{x} - \vec{R}|) \times \begin{cases} \omega_2(|\vec{x} - \vec{R}|) - \beta j_2(\alpha |\vec{x} - \vec{R}|), & |\vec{x} - \vec{R}| < A, \\ 0, & |\vec{x} - \vec{R}| > A, \end{cases} \quad (\text{IV3})$$

where β and α are chosen so that φ and its first derivative vanish at A , and ω_2 is the $l=2$ solution to Schrödinger's equation with no nodes and zero slope at A . These nonoverlapping d functions allow Caruthers and Kleinman to use a manageable set of standing waves in the expansion of the eigenfunctions of the slab.

Caruthers and Kleinman used three differently constructed potentials in order to explore the sensitivity of their results to the details of the potential. The most realistic (with regards to both bulk and surface properties) was constructed by superposing atomic $3d^4 4s^1$ Coulomb potentials and calculating the exchange and correlation potential by overlapping atomic densities and using Slater's $\rho^{1/3}$ (Slater, 1951). In addition the $4s$ electrons were modified by modulating their tails in the vacuum region so that the experimental work function was obtained.

The spectrum of the Fe slab for this as well as three other choices for the potential were studied (at $\vec{k}_{||} = 0$). They find two surface states which are s - d hybrids in general agreement with Kasowski's work on W and Mo (Kasowski, 1975).

The higher of the two surface states found at Γ lies 1.5 eV below the Fermi level and is well located within the surface region. It is shown in Fig. 17. They find their calculated spectrum is sensitive to the details of the surface potential and conclude that self-consistency is important to include in transition metal surface-state studies.

V. CHEMISORPTION

A. Introduction

A very large theoretical effort is being made to calculate the chemical and electronic properties of chemi-

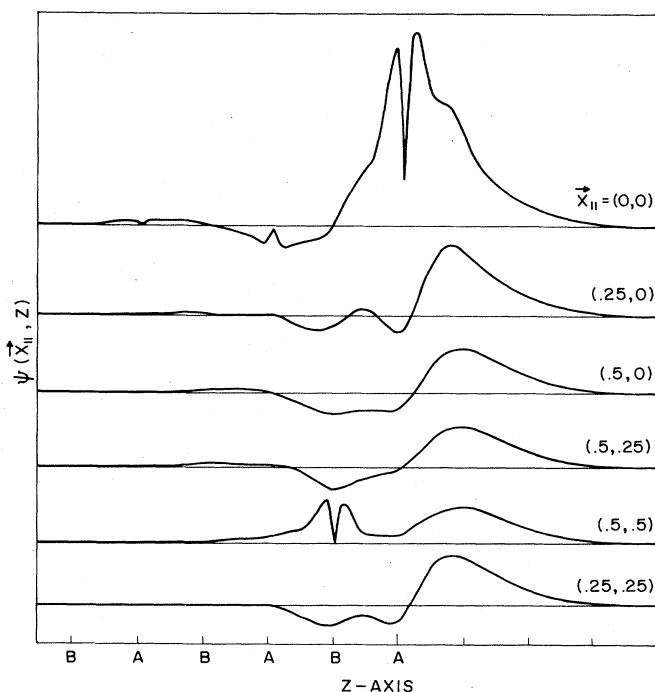


FIG. 17. Surface state wave function for the Fe(100) surface at energy -0.27 Ry measured from the Fermi level plotted along several rays normal to the surface. The ray $(0,0)$ passes through a first layer atom, and $(1/2, 1/2)$ passes through a second layer atom. Core region oscillations have been removed from the figure. From Caruthers and Kleinman (1975), with permission.

sorbed systems. We shall restrict ourselves to those which treat an ordered overlayer of foreign atoms on a surface, and not discuss the problem of an isolated chemisorbed atom on a surface. We focus on two quite different systems, H chemisorbed on Si(111), for which calculations have been carried out by Appelbaum and Hamann (1975b), using the self-consistent field method, and Pandey (1976), using the semiempirical tight-binding approach, and the work of Kasowski (1974) for the O on Ni(100) system, carried out using the LCMTO method described in Sec. IV.

B. H on Si(111)

Using the method described in Sec. II.B, Appelbaum and Hamann (1975b) have studied the electronic properties of H on Si(111). They have calculated density of states in the surface region, the strength of the Si-H bond, and the equilibrium spacing between the Si and H overlayer. Atomic hydrogen chemisorbs on the Si(111), saturating the single broken bond per surface atom present on this surface (Ibach and Rowe, 1974). This removes the dangling bond surface-state band and replaces it by a band of states that, over large portions of $\vec{k}_{||}$ space, hybridizes strongly with the energy level structure of Si substrate. Where it exists as a surface state the Si-H bond looks like a strongly polarized s wave. The charge density in the Si-H bond surface state is exhibited at a particular point in $\vec{k}_{||}$ space in Fig. 18.

The spectrum on the H atom is plotted in Fig. 19, together with the bulk density of states of the Si substrate. Notice the suppression of most of the s band and the enhancement of the lower portion of the p band and the top of the s band. The calculated density of states and measured photoemission spectra are in close agreement, as seen in Fig. 20, where the difference between the bulk Si density of states and that on the H are compared with the data taken by Sakurai and Hagstrum (1975). From studies of the force on the H plane, via the Hellmann-Feynman theorem (Hellman, 1937; Feynman, 1937), an equilibrium position and force constant for the

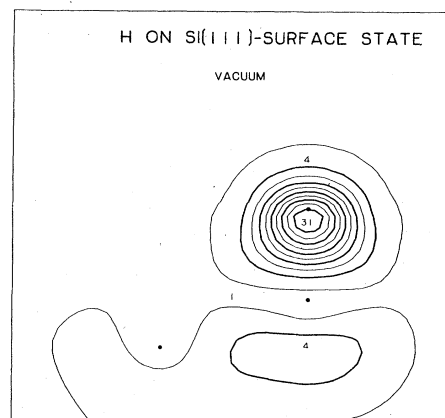


FIG. 18. Contours of constant charge density for a surface state on the Si(111) surface with chemisorbed H. The state is at ~ -5 eV relative to the valence band maximum. The H atom and Si atoms in the first two layers are indicated by dots. From Appelbaum and Hamann (1975b).

Si-H bond is obtained. The calculated force constant is 0.175 (a.u.), which implies a Si-H vibration mode that agrees with that measured by infrared absorption within 5% (Becker and Gobeli, 1963). The calculated Si-H bond length agrees within 0.03 Å with the experimental Si-H bond length extracted from molecular studies on a large variety of Si-H compounds.

Pandey (1976) has studied H on Si with an empirical tight-binding method, described in Sec. III.A. The parameters of his model were fixed in the following ways. The Si-Si overlap parameters were fixed from their study of bulk Si as in Sec. III.A, while the Si-H overlap and diagonal energy splittings were determined by fitting the molecular spectra of silane (SiH_4) and disilane (Si_2H_6). He obtains a density of states on the H similar to that shown in Fig. 20 obtained by Appelbaum and Hamann, and in excellent agreement with experiment.

C. O on Ni(100)

Kasowski (1974), using the LCMTO method, has studied surface states induced by O chemisorbed on Ni in a perfect 1×1 overlayer and placed 0.9 Å above the Ni surface layer. He finds that O induces surface states of p character at -0.4 Ry and -0.55 Ry (referenced to the Fermi energy). The state at -0.4 Ry has been seen in INS and UPS and identified by Hagstrum and Becker (1969) as a p state from their study of the O, S, and Se on Ni series. While the experiments were performed on a $C(2 \times 2)$ structure, Kasowski argues that the small overlap of the oxygens, even on the 1×1 form, make the theoretical conclusions found for 1×1 applicable to the $C(2 \times 2)$ form. Kasowski studied the dependence of the surface-state spectra on changes in d , the O-Ni layer spacing, and concluded that the spectra for $d=0.9$ Å, the spacing predicted by Demuth *et al.* (1973) from LEED studies, was in much better agreement with the experimental spectra than the choice $d=1.5$ Å, predicted

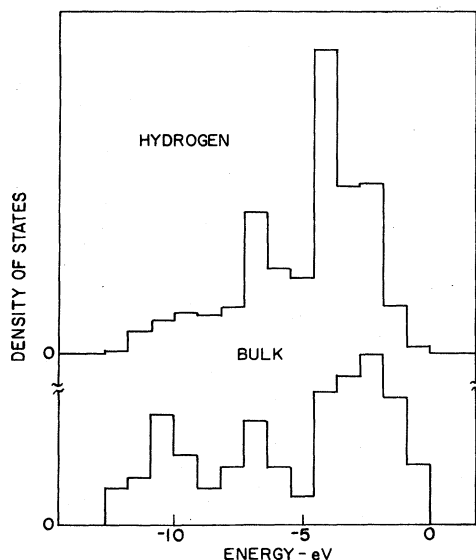


FIG. 19. Local density of states on H for H chemisorbed on Si(111) compared to the bulk Si density of states. From Appelbaum and Hamann (1975b).

by Anderson *et al.* (1973), also from LEED. Presently, the LEED studies by different workers have converged on $d=0.9$ Å, so that there is general agreement between LEED inferred geometries and that inferred from experimental and theoretical spectral comparisons.

VI. SUMMARY

The examples discussed in the preceding sections present a stopped-motion snapshot of a rapidly moving field. It is safe to speculate that by the time this article is in the readers' hands, a number of additional studies will have been carried out by the researchers represented here, and that comparable or better calculations by others will have appeared based on similar or new methods.

In both discussing the existing calculations and projecting trends into the future, one must keep in mind that surface calculations exist between two well-established bodies of work. On the one side are calculations of the electronic structures of bulk solids, and on the other, molecular calculations. It is unlikely that any fundamentally new approximations or types of representation for wave functions are going to be initially developed in the surface context. The process so far has primarily been one of selecting elements from the other contexts which are most suitable for surface problems. Lacking some of the simplifying symmetry properties of bulk solids, or the small number of atoms of most molecules that have been studied in a first-principles fashion, computational efficiency has been an important factor guiding the choices. As a result, pseudopotentials

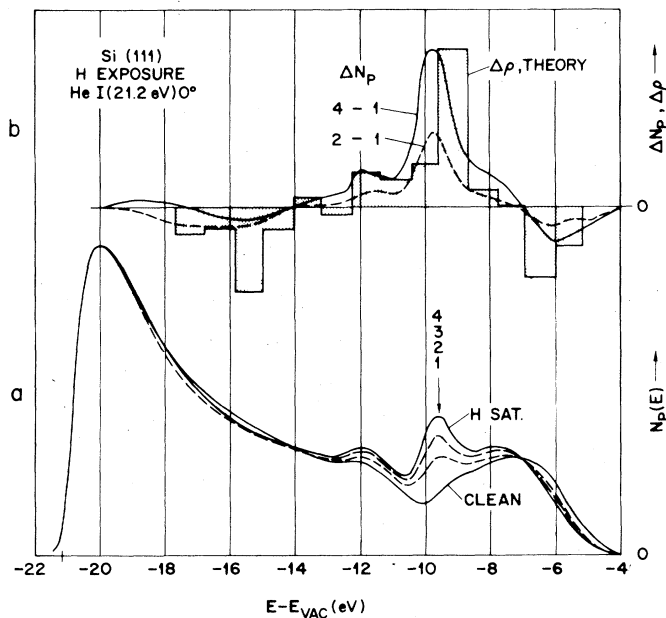


FIG. 20. uv photoemission spectrum at $\hbar\omega=21.2$ eV for clean Si(111) and Si(111) after varying degrees of H exposure. Top inset shows difference curves compared to difference histogram of the theoretical densities of states in Fig. 19. From Sakurai and Hagstrum (1975), with permission.

have been heavily employed, and the local approximation for the exchange-correlation potential is nearly universal. These are certainly among the most efficient and accurate approximations employed in bulk band theory. On the other hand, considerably greater emphasis is being placed on self-consistency than is customary in bulk calculations, the surface field being closer to molecular studies in this respect. This is motivated by the fact that no other way exists to determine how rapidly the disturbance produced by the surface is screened out, and what charge and potential distortions accompany the geometrical distortions present at many surfaces. Self-consistency is also absolutely necessary if calculations of equilibrium surface geometries are to become common.

It is clear that in computational efficiency alone, minimum-basis empirical tight-binding schemes excel. The limitations on these schemes are primarily imposed by problems in choosing the parameters. In the examples cited here, very good results were obtained for semiconductors and chemisorption on semiconductors. On the other hand, there are many (uncited) examples where such schemes have produced results considerably inferior in quantitative accuracy. Further exploration of the extent to which the principles employed in parameter selection in the cited examples will continue to be successful in a wider range of systems is clearly desirable. One may also anticipate a hybrid type of approach in which first-principles calculations are used to fit empirical parameters in bonding situations that have no convenient solid state or molecular analog (or no available data) and these parameters then used to treat a surface situation too complex to be computationally tractable in a first-principles scheme.

The preponderance of calculations reported here is based on a slab geometry rather than a semi-infinite geometry. As discussed in Sec. I.B, the physical information available is really the same in both cases. The slab methods are generally more easily programmed, since the bulk of the calculation is a matrix diagonalization, while the semi-infinite methods can generally get more out of a given amount of computer capacity. The ability to work back and forth between the two with a common set of approximations would be valuable, since this would, for example, enable one to achieve self-consistency with a coarse mesh of states, and then examine interesting spectral features in fine-grained detail.

The final point to consider is an overall question: to what ends are all the efforts that have been discussed here directed? First, toward the development of methods sufficiently accurate to provide reliable quantitative aid in the interpretation of a variety of surface experiments. Second, toward an understanding of the additional physical and chemical effects that are peculiar to the surface, and to identify the key parameters in terms of which these effects may be empirically systemized. Finally, to offer calculational insights into physical and chemical structures that are not accessible to direct experimental measurement, such as intermediate surface transition states, which are important for catalytic reactions.

REFERENCES

- Allredge, G. P. and L. Kleinman, 1974a, *Phys. Rev. B* **10**, 559.
 Allredge, G. P. and L. Kleinman, 1974b, *Phys. Lett. A* **48**, 337.
 Allredge, G. P. and L. Kleinman, 1974c, *J. Phys. F* **4**, L207.
 Andersen, O. K. and R. V. Kasowski, 1971, *Phys. Rev. B* **4**, 1063.
 Andersen, S., B. Kasema, J. B. Pendry, and M. A. van Hove, 1973, *Phys. Rev. Lett.* **31**, 595.
 Animalu, A. O. E. and V. Heine, 1965, *Phil. Mag.* **12**, 249.
 Appelbaum, J. A. and D. R. Hamann, 1972, *Phys. Rev. B* **6**, 2166.
 Appelbaum, J. A. and D. R. Hamann, 1973, *Phys. Rev. Lett.* **31**, 106.
 Appelbaum, J. A. and D. R. Hamann, 1974, *Phys. Rev. Lett.* **32**, 225.
 Appelbaum, J. A. and D. R. Hamann, 1975a, *Phys. Rev. B* **12**, 1410.
 Appelbaum, J. A. and D. R. Hamann, 1975b, *Phys. Rev. Lett.* **34**, 806.
 Appelbaum, J. A., G. A. Baraff, and D. R. Hamann, 1975a, *Phys. Rev. B* **11**, 3822.
 Appelbaum, J. A., G. A. Baraff, and D. R. Hamann, 1975b, *Phys. Rev. B* **12**, 5749.
 Appelbaum, J. A., G. A. Baraff, and D. R. Hamann, 1975c, *Phys. Rev. Lett.* **35**, 729.
 Appelbaum, J. A., G. A. Baraff, and D. R. Hamann, 1976, *Phys. Rev.* (to be published).
 Appelbaum, J. A. and E. I. Blount, 1973, *Phys. Rev. B* **8**, 483.
 Ashcroft, N. W., 1966, *Phys. Lett.* **23**, 48.
 Becker, G. E. and G. W. Gobeli, 1963, *J. Chem. Phys.* **38**, 2942.
 Calandra, C. and G. Santoro, 1975, *J. Phys. C* **8**, L86.
 Callcott, T. A. and A. U. MacRae, 1969, *Phys. Rev.* **178**, 966.
 Caruthers, E. and L. Kleinman, 1975, *Phys. Rev. Lett.* **35**, 738.
 Chelikowsky, J. R., M. Schlüter, S. G. Louie, and M. L. Cohen, 1975, *Solid State Commun.* **17**, 1103.
 Chelikowsky, J. R. and M. L. Cohen, 1976, *Phys. Rev.* **13**, 826.
 Cohen, M. L., M. Schlüter, J. R. Chelikowsky, and S. G. Louie, 1975, *Phys. Rev. B* **12**, 5575.
 Davison, S. G. and J. D. Levine, 1970, in *Solid State Physics*, edited by H. Ehrenreich, F. Seitz, and D. Turnbull (Academic, New York), Vol. 25, p. 1.
 Demuth, J. E., D. W. Jepsen, and P. M. Marcus, 1973, *Phys. Rev. Lett.* **31**, 540.
 Dresselhaus, G. and M. S. Dresselhaus, 1967, *Phys. Rev.* **160**, 649.
 Eastman, D. E. and M. I. Nathan, 1975, *Phys. Today* (April) **28**, 44.
 Feynman, R. P., 1939, *Phys. Rev.* **56**, 340.
 Forstmann, F. and V. Heine, 1970, *Phys. Rev. Lett.* **24**, 1419.
 Forstmann, F. and J. B. Pendry, 1970, *Z. Phys.* **235**, 69.
 Garcia, N., 1975, *Solid State Commun.* **17**, 397.
 Hagstrum, H. D. and G. E. Becker, 1969, *Phys. Rev. Lett.* **22**, 1054.
 Haneman, D., 1961, *Phys. Rev.* **121**, 1093.
 Heine, V., 1962, *Proc. Phys. Soc. Lond.* **81**, 300.
 Hellman, H., 1937, *Einführung in die Quantum Theorie* (Deuticke, Leipzig), p. 285.
 Herman, F. and S. Skillman, 1963, *Atomic Structure Calculations* (Prentice Hall, Englewood Cliffs, N. J.).
 Herring, C., 1966, in *Magnetism*, edited by G. T. Rado and H. Suhl (Academic, New York), Vol. 4.
 Hirabayashi, K., 1969, *J. Phys. Soc. Jpn.* **27**, 1475.
 Ibach, H., 1971, *Phys. Rev. Lett.* **27**, 253.
 Ibach, H. and J. E. Rowe, 1974, *Surf. Sci.* **43**, 481.

- Jepsen, D. W. and P. M. Marcus, 1971, in *Computational Methods in Band Theory*, edited by P. M. Marcus, J. F. Janak, and A. R. Williams (Plenum, New York), p. 417.
- Joannopoulos, J. D. and M. L. Cohen, 1974, *Phys. Rev. B* **10**, 5075.
- Jones, R. O., 1968, *Phys. Rev. Lett.* **20**, 992.
- Jones, R. O., 1975, in *Surface Physics of Semiconductors and Phosphors*, edited by C. G. Scott and C. E. Reed (Academic, London), p. 96.
- Kasowski, R. V., 1974, *Phys. Rev. Lett.* **33**, 1174.
- Kasowski, R. V., 1975, *Solid State Commun.* **17**, 179.
- Kittel, C., 1963, *Quantum Theory of Solids* (Wiley, New York).
- Kohn, W. and N. Rostoker, 1954, *Phys. Rev.* **94**, 111.
- Kohn, W. and L. J. Sham, 1965, *Phys. Rev.* **140**, A1133.
- Korringa, J., 1947, *Physica (Utrecht)* **13**, 392.
- Lang, N. D., 1973, in *Solid State Physics*, edited by H. Ehrenreich, F. Seitz, and D. Turnbull (Academic, New York), Vol. **28**, p. 225.
- Lang, N. D. and W. Kohn, 1970, *Phys. Rev. B* **1**, 4555.
- Lang, N. D. and W. Kohn, 1971, *Phys. Rev. B* **3**, 1215.
- von Laue, M., 1931, *Phys. Rev.* **37**, 53.
- Löwdin, P., 1951, *J. Chem. Phys.* **19**, 1396.
- Marcus, P. M. and D. W. Jepsen, 1968, *Phys. Rev. Lett.* **20**, 925.
- Pandey, K. C., 1976, *Phys. Rev. B* (to be published).
- Pandey, K. C. and J. C. Phillips, 1974a, *Phys. Rev. Lett.* **32**, 1433.
- Pandey, K. C. and J. C. Phillips, 1974b, *Solid State Commun.* **14**, 439.
- Pandey, K. C. and J. C. Phillips, 1975, *Phys. Rev. Lett.* **34**, 1451.
- Pandey, K. C. and J. C. Phillips, 1976, *Phys. Rev. B* **13**, 750.
- Park, R. L., 1975, *Phys. Today (April)* **28**, 52.
- Pines, D., 1962, *The Many-Body Problem* (Benjamin, New York).
- Phillips, J. C., 1973, *Surf. Sci.* **40**, 459.
- Plummer, E. W., J. W. Gadzuk, and D. R. Penn, 1975, *Phys. Today (April)* **28**, 63.
- Rowe, J. E., 1974, *Phys. Lett. A* **46**, 400.
- Rowe, J. E. and H. Ibach, 1974, *Phys. Rev. Lett.* **32**, 421.
- Sakurai, T. and H. D. Hagstrum, 1975, *Phys. Rev. B* **12**, 5349.
- Schlier, R. E. and H. E. Farnsworth, 1959, *J. Chem. Phys.* **30**, 917.
- Schlüter, M., J. R. Chelikowsky, S. G. Louie, and M. L. Cohen, 1975, *Phys. Rev. Lett.* **34**, 1385.
- Schrieffer, J. R. and P. Soven, 1975, *Phys. Today (April)* **28**, 24.
- Slater, J. C., 1951, *Phys. Rev.* **81**, 385.
- Wigner, E. P., 1934, *Phys. Rev.* **46**, 1002.